Inflamm. Res. (2017) 66:725–737
DOI 10.1007/s00011-017-1053-3

Inflammation Research

ORIGINAL RESEARCH PAPER

Anethole reduces inflammation and joint damage in rats with adjuvant-induced arthritis

Alessandra Mileni Versuti Ritter[1,4] · Luzmarina Hernandes[2] · Bruno Ambrosio da Rocha[3] · Camila Fernanda Estevão-Silva[3] · Edirlene Sara Wisniewski-Rebecca[3] · Joice dos Santos Cezar[3] · Silvana Martins Caparroz-Assef[3] · Roberto Kenji Nakamura Cuman[3] · Ciomar Aparecida Bersani-Amado[3]

Received: 26 January 2017 / Revised: 18 April 2017 / Accepted: 3 May 2017 / Published online: 25 May 2017

Abstract
Aim This study evaluated whether anethole attenuates the inflammatory response and joint damage in a model of adjuvant-induced arthritis (AIA) in rats.
Methods The animals were treated with 62.5-, 125-, or 250-mg/kg anethole daily for 21 days after AIA and necropsied on days 14 and 21 to evaluate the number of serum and synovial leukocytes (total and differential), serum cytokines (IL-2, IL-6, IL-12, IL-17, and TNF-α), and nitric oxide concentrations. Morphologic changes in the cartilage and bone of the femorotibial articulation in both left paw and right paw were studied in hematoxylin/eosin and Sirius Red-hematoxylin sections.
Results Different doses of anethole suppressed paw swelling and the number of serum and synovial leukocytes. However, 250 mg/kg of anethole more effectively controlled local and systemic inflammation. Histological evaluation revealed significant prevention of cartilage damage and inflammatory infiltrate scores. Morphometric analysis showed pannus formation, the thickness of the articular cartilage, and bone resorption lower in the anethole-treated AIA group compared to untreated AIA group on both days 14 and 21. These significant anti-inflammatory effects in the anethole-treated AIA group were associated with downregulation of cytokines and nitric oxide levels.
Conclusion Therefore, anethole may be a useful intervention to treat inflammatory arthritis.

Keywords Anethole · Adjuvant-induced arthritis · Anti-inflammatory effect · Cytokines

Responsible Editor: Bernhard Gibbs.

✉ Alessandra Mileni Versuti Ritter
ale_mileni@hotmail.com

[1] Laboratory of Pharmacology Cardiovascular, Faculty of Medical Sciences, University of Campinas, Campinas, SP, Brazil

[2] Department of Morphology Science, State University of Maringá, Maringá, PR, Brazil

[3] Department of Pharmacology and Therapeutics, State University of Maringá, Maringá, PR, Brazil

[4] Rua Alexandre Fleming, 105, Campinas, SP 13084-971, Brazil

Introduction

Rheumatoid arthritis (RA) is a chronic immune-mediated disease that is characterized by a severe inflammatory process. The major alterations include hypertrophy and hyperplasia of the synovial lining and increased synovial fluid volume. If left untreated, RA can lead to irreversible damage to adjacent cartilage and bone. Interactions between local cells and recruited inflammatory cells release inflammatory mediators [1], such as cytokines (tumor necrosis factor α [TNF-α], interleukin 1β [IL-1β], IL-6, and IL-17) [2], that increase the damage. Moreover, synthesis of matrix proteolytic enzymes and osteoclast activation [3] are also responsible for bone and cartilage damage. Therefore, inflammatory process might be responsible for the development and maintenance of local and clinical disease manifestations [1, 3].

The conventional treatments for arthritis comprise steroidal and non-steroidal anti-inflammatory drugs, disease-modifying anti-rheumatic drugs, and immunosuppressant drugs that transiently suppress inflammation and attenuate symptoms through different mechanisms of action. However, they do not treat the disease in the long term and

frequently have serious side effects [4–6]. Thus, newer and safer drugs to treat RA with low or no toxicity and beneficial effects are under scientific investigation. Many medicinal plants have actively been sought to develop a promising drug in this field [7].

Anethole (1-methoxy-4-[(E)-propenyl]-benzene) is the major and active component (80–90%) of essential oils of anise (*Illicium verum*) [8]. It is an aromatic compound that is traditionally used in pharmaceutical formulations because of its antioxidant, gastroprotective, and hepatoprotective effects [9, 10]. A recent study by our group demonstrated that anethole has antinociceptive and anti-inflammatory activity in different experimental models of acute inflammation [11, 12]. To date, however, no studies have reported its effects on chronic inflammatory disease.

Adjuvant-induced arthritis (AIA) in rats is a valuable experimental model that causes an intense and persistent inflammatory response that is similar to RA in humans [13–16]. Indeed, the high similarity between the AIA model and RA allows us to use this model to study new drugs to treat this disease [17]. The aim of the present study was to investigate the effects of oral anethole administration on systemic and articular inflammation in a rat model of AIA and the possible mechanism of action.

Materials and methods

Animals

Male Holtzman rats, weighing 200–220 g, were used in this study. They were kept in cages in a temperature-controlled room on a 12/12-h light/dark cycle with ad libitum access to food and water. These rat strains, more readily available to us, develop severe and low variable arthritis clinical signs at 100% incidence [18, 19]. All of the procedures and protocols were approved by the Committee for Animal Studies of the State University of Maringá (125/2010—CEEA).

Induction of arthritis and treatment of rats

Arthritis was induced in rats by a single subcutaneous injection of 0.1 mL of a Complete Freund's Adjuvant suspension (killed and dried *Mycobacterium tuberculosis* suspended in mineral oil; Nujol®, Schering-Plough, São Paulo, Brazil) at a concentration of 0.5% (w/v) into the left hind paw. The animals were randomly divided into five groups: (1) normal group, (2) untreated AIA group, (3) AIA group treated with 62.5 mg/kg anethole (Sigma-Aldrich, St. Louis, MO, USA), (4) AIA group treated with 125 mg/kg anethole, and (5) AIA group treated with 250 mg/kg anethole. The treatment was performed by gavage beginning on the day of AIA induction (day 0) and then once daily for 21 days. The control group and untreated AIA group were treated with water (vehicle) orally for 21 days.

Clinical parameters: hind paw volume and arthritis score

The development of AIA was assessed by paw volume changes and the appearance of secondary lesions. The volume of the injected and non-injected hind paw was assessed by digital plethysmography (UgoBasile®). The results are expressed as an increase in paw volume that was recorded on day 1, 3, 6, 9, 13, 17, and 21 compared with the initial volume. The severity of secondary lesions was evaluated by a numerical grading system, as reported by Rosenthale [20]. This was done by assigning points to each of the following events: appearance of nodules in the tail (+1), appearance of nodules in one or both ears (+1 or +2), and occurrence of swelling in one or both forelimbs (+1 or +2). The severity of these secondary lesions was graded from 0 to 5, in which 0 indicated the absence of lesions. This evaluation was performed daily from day 10 of arthritis induction. Finally, on days 14 and 21, the animals were euthanized, and samples of blood, synovial fluid, and femorotibial articulations were collected for later analysis.

Total and differential articular leukocytes

Synovial fluid was collected on days 0, 14, and 21 after arthritis induction to obtain the total and differential counts of circulating and articular leukocytes. The femorotibial joints were exposed by surgical section of the patellar tendon. The articular cavity was then washed with 40 μL of phosphate-buffered saline (PBS)/EDTA solution and the total number of leukocytes was determined using a Neubauer hemocytometer chamber. The differential cell count was performed with blood smears that were fixed and stained using the May–Grunwald–Giemsa panchromatic method. Cellular characterization was performed using an optical microscope with an oil immersion objective.

Measurement of cytokines

Blood samples were collected on days 14 and 21 after arthritis induction to measure cytokine concentrations. The blood samples were centrifuged, and the supernatants (serum) were collected and stored at −70 °C for the subsequent determination of IL-2, IL-6, IL-12, IL-17, and TNF-α levels. Cytokine levels were quantified using magnetics assay kit (Invitrogen™ multiplex assays for the Luminex™ platform) according to the manufacturer's instructions.

Measurement of nitrite

Blood samples were collected on days 14 and 21 after arthritis induction to determine indirectly the nitric oxide (NO) levels by nitrite concentration in the samples. The blood samples were centrifuged at 700×*g* for 15 min, and the supernatants (serum) were stored at −70 °C for the subsequent determination of nitrite levels, which were measured by the Griess method. The concentration was calculated according to the standard curve of sodium nitrite. The results are expressed as μg/mL.

Articular histology evaluation

Fourteen and twenty-one days after arthritis induction and treatment with 250 mg/kg anethole, the animals were euthanized. The right and left femorotibial articulations were collected and immediately fixed in 10% formalin for 48 h. The articulations were decalcified in 10% ethylenediaminetetraacetic acid (pH 7.4) for 21 days. The articulations were then dehydrated and embedded in paraffin blocks. Semi-serial 6-μm-thick slices were stained with hematoxylin/eosin or Sirius Red-hematoxylin. All of the histological sections were tested.

The histological assessment of inflammatory infiltration, the score of other symptoms of inflammation in the synovial membrane and periarticular tissues, and the score of cartilage damage were performed by two independent researchers in a blinded manner. To classify the intensity of lymphocytic infiltration in the synovial membrane, a 5-point scale (0–4) was used: 0 (absence of inflammatory cells with normal synovial membrane), 1 (low inflammatory cells scattered across the tissue), 2 (moderate inflammatory cells scattered across the tissue with small groups of cells), 3 (high inflammatory cells distributed throughout the tissue), and 4 (high inflammatory cells distributed throughout the tissue with evident membrane thickening).

To classify cartilage damage, a 6-point scale (0–5) was used: 0 (absence of damage), 1 (increased number of chondrocytes distributed in columns), 2 (increased number of chondrocytes distributed in columns and also disorganized chondrocytes), 3 (decreased number of chondrocytes with disorganized distribution), 4 (change in the number of chondrocytes and disorganized articular membrane superficies), and 5 (change in the number of chondrocytes, disorganized articular membrane superficies, and pannus formation in articular cartilage).

To determine the thickness of the synovial membrane and cartilage, morphometric analysis was conducted to measure the right and left synovial membrane of the femur and tibia. These analyses were performed using an optical microscope (Olympus BX41, Olympus, Tokyo, Japan) with ×4 (synovial membrane) and ×10 (cartilage) objectives. To determine the synovial membrane thickness, 45 measurements were made per group (three random measurements per slice for a total of nine analyses per animal). To determine tibial and femoral cartilage thickness, 15 measurements were made for each femoral and tibial cartilage section (five random measurements per slice in three slices per animal for a total of 90 measurements per group).

The Sirius Red-hematoxylin-stained sections were used to determine the organic matrix area on subcondral bone that underlies the articulation of the tibia and femur. Three random points were measured per histological section (nine measurements per animal per tibia subcondral bone and nine measurements per animal per femur subcondral bone) using a polarized light microscope with a ×20 objective. Tissue images were collected with a Nikon Ds-FilC digital camera (Minato-ku, Tokyo, Japan) attached to a Nikon Eclipse 80I microscope (Nikon, Tokyo, Japan). The area algorithm was based on the pixel area of the organic bone matrix using ImagePro 4.5 software (Media Cybernetics, Silver Spring, MD, USA). The values for the tibia and femur are expressed together, indicating the organic matrix area (μm^2) on subcondral bone that underlies the right and left articulation.

Statistical analysis

The results are expressed as mean ± standard error of the mean (SEM) and were analyzed using *t* tests or analysis of variance (ANOVA), followed by Tukey's post hoc test. The level of significance was 5%. The data were analyzed using Prism 4.0 software (GraphPad, San Diego, CA, USA).

Results

Clinical parameters: hind paw volume and arthritis score

Figure 1 shows the volume in the left (Fig. 1a) and right (Fig. 1b) paws in normal animals, arthritic animals, and arthritic animals treated with anethole at doses of 62.5, 125, and 250 mg/kg. The subcutaneous injection of CFA in the left paw induced an inflammatory reaction 24 h after administration. The inflammatory response remained constant until day 9. Afterward, a progressive increase in paw volume was observed in left injected and right non-injected paws until day 21 (Fig. 1a, b). The increase in paw volume in normal animals was regarded as negligible. Anethole at doses of 125 and 250 mg/kg reduced the volume of the injected paw by 41, 28, and 40% on days 9, 17, and 21 after

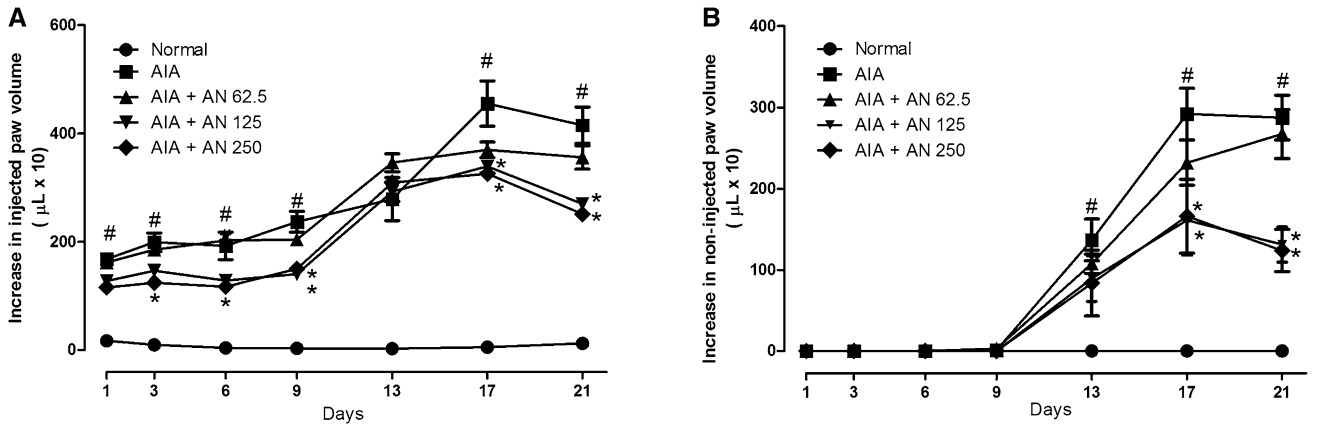

Fig. 1 Effect of anethole (62.5, 125, and 250 mg/kg) on *left injected* (**a**) and *right non-injected* (**b**) paws volume 0, 1, 3, 6, 9, 13, 17, and 21 days after the induction of adjuvant-induced arthritis. Anethole was administered daily, orally, beginning on the same day as arthritis induction. The data are expressed as the mean ± SEM. *Vertical bars* represent standard errors of the means. The data are expressed as the mean ± SEM of 10 animals for each experimental group. *$p < 0.05$, compared with normal group (one-way ANOVA followed by Tukey test)

AIA, respectively. No significant difference was found between the 125 and 250 mg/kg doses of anethole. In addition, 250 mg/kg anethole reduced the paw volume decreasing 40 and 37% on days 3 and 6 after arthritis induction. In the non-injected paw, 125 and 250 mg/kg anethole significantly reduced the progression of the inflammatory process by 43 and 57% on days 17 and 21 after arthritis induction, respectively. No significant difference was found between the anethole doses of 125 and 250 mg/kg. Treatment with 62.5 mg/kg anethole did not result in significant improvements in the non-injected paw.

Secondary lesions began to appear on day 10 after arthritis induction, with a maximum score of 5 points on day 14. Treatment with 125 mg/kg anethole after arthritis induction delayed the appearance of secondary lesions. Treatment with 250 mg/kg anethole delayed the appearance of secondary lesions and also decreased secondary lesions from day 11 to day 14 after arthritis induction. Treatment with 62.5 mg/kg anethole after arthritis induction did not change this parameter (Table 1). The macroscopic analysis showed that all of the animals that were treated with anethole, independent of the doses used, had milder secondary lesions compared with the untreated AIA group.

Total and differential articular leukocytes

Figure 2 shows the variation in the leukocyte population in synovial joint fluid in normal animals and arthritic animals untreated and treated with anethole at doses of 62.5, 125, and 250 mg/kg on day 14 (Fig. 2a, c, e) and day 21 (Fig. 2b, d, f) after the CFA injection. The average number of leukocytes in the left and right articular cavity before arthritis induction was approximately 2000/cavity, with a predominance of mononuclear cells (70%) relative to polymorphonuclear cells (30%). After arthritis induction, the total number of leukocytes significantly increased in the left and right synovial fluids in arthritic rats. The number of leukocytes increased approximately tenfold in the right synovial cavity and 40-fold in the left synovial cavity on days 14 and 21, respectively. These increases in the number of total leukocytes were attributable to an increase in both cell types but especially polymorphonuclear cells. Treatment with 125 and 250 mg/kg anethole significantly decreased the total number of leukocytes, mononuclear cells, and polymorphonuclear cells compared with the untreated AIA group on days 14 and 21. Treatment with 62.5 mg/kg anethole did not reduce the increase in the number of leukocytes on either day of analysis.

Cytokine levels: anethole downregulated pro-inflammatory cytokine levels in AIA rats serum

We observed better anti-inflammatory effects of 250 mg/kg anethole treatment compared with the other doses. Therefore, we further analyzed cytokines and performed histological analyses using only this dose.

Figure 3 shows the general features of cytokine levels on days 14 and 21 after arthritis induction. No differences were observed in IL-2 (Fig. 3a), IL-6 (Fig. 3c), or TNF-α (Fig. 3e) levels between the normal and AIA groups 14 days after arthritis induction. The levels of IL-1α (Fig. 3a) and IL-17 (Fig. 3d) were higher in the AIA group than in the normal group. The levels of IL-6, IL-17, and TNF-α were higher in the AIA group on day 21 after arthritis induction compared with the normal group. Animals that were treated with 250 mg/kg anethole had lower IL-1α and IL-17 levels than the untreated AIA group on

Table 1 Effect of anethole (62.5, 125, or 250 mg/kg) on secondary lesion scores after the induction of adjuvant-induced arthritis

	Day after AIA											
	10	11	12	13	14	15	16	17	18	19	20	21
AIA ($n = 10$)	0 (0–4)	2 (1–5)	3 (2–5)	4 (3–5)	5 (5–5)	5 (5–5)	5 (5–5)	5 (5–5)	5 (5–5)	5 (5–5)	5 (5–5)	5 (5–5)
AN 62.5 ($n = 10$)	1 (0–3)	3 (0–4)	4 (0–5)	5 (2–5)	5 (4–5)	5 (4–5)	5 (4–5)	5 (4–5)	5 (5–5)	5 (5–5)	5 (5–5)	5 (5–5)
AN 125 ($n = 10$)	0 (0–1)	1 (0–2)	2 (0–5)	3 (1–5)	4 (1–5)	4 (3–5)	4 (4–5)	5 (4–5)	5 (4–5)	5 (4–5)	5 (4–5)	5 (4–5)
AN 250 ($n = 10$)	0 (0–2)	0 (0–3)*	2 (0–4)*	3 (0–5)*	3 (0–5)*	4 (3–5)	4 (3–5)	4 (3–5)	4 (3–5)	4 (3–5)	4 (3–5)	4 (3–5)

The evaluation of secondary lesions occurred daily and was initiated on day 10 after the induction of adjuvant-induced arthritis. The severity of secondary lesions was graded from 0 to 5, in which 0 indicated the absence of lesions. This was done by assigning points to each of the following events: appearance of nodules in the tail (+1), appearance of nodules in one or both ears (+1 or +2), and occurrence of swelling in one or both forelimbs (+1 or +2). Anethole (AN) was administered at doses of 62.5, 125, and 250 mg/kg. The data are expressed as median (range) for each group

n number of animal for each experimental group, *AIA* adjuvant-induced arthritis

* $p < 0.05$, compared with AIA group (one-way ANOVA followed by Tukey test)

day 14 after arthritis induction. No differences were found in the levels of the other cytokines. We observed decreases in the levels of IL-2, IL-6, IL-17, and TNF-α in the anethole-treated AIA group compared with the untreated AIA group on day 21 after arthritis induction.

Nitrite levels: anethole downregulated nitrite level in AIA rats serum

The levels of nitrite were similar on days 14 and 21 in the normal group. The levels of nitrite on days 14 and 21 after arthritis induction were higher in the AIA group compared with the normal group (Fig. 4). Nitrite levels increased approximately sixfold on day 14 and twofold on day 21 after arthritis induction. Treatment for 14 and 21 days with 250 mg/kg anethole significantly reduced nitrite levels by 29 and 54%, respectively.

Articular histology evaluation

Typical photomicrographs of knee joint sections that were stained with hematoxylin/eosin illustrated the severity of joint damage. Histological analyses were performed to investigate whether anethole relieved damage in the knee joint in AIA rats. In the normal group, the articular cartilage had smooth surfaces with intact layers, with no inflammation or bone destruction (Fig. 5a–c). In the arthritic group, the knee joints presented severe alterations in both periods analyzed (days 14 and 21) (Fig. 5d–g). These alterations were characterized by cartilage depletion, obvious underlying bone destruction, and severe inflammatory cell infiltration on both days. We observed an increase in the number of chondrocytes that were distributed in columns (Fig. 5f) and an increase in the thickness of cartilage in both the left tibia and femur on day 14 (Fig. 5d, thin arrows) and in the right joint on day 21 after arthritis induction. The left tibia presented a decrease in the number of chondrocytes on day 21 and thinning of the cartilage with pannus formation in the cartilage (Fig. 5d, e, thick arrows). Both the right and left synovial membrane presented hyperplasia and hypertrophy of synovial cells, with severe inflammatory infiltration, resulting in pannus formation on day 14 (Fig. 6c, e) and day 21 (Fig. 6g, i). Compared with untreated AIA rats, 250 mg/kg anethole ameliorated the aforementioned pathological changes to varying degrees. The right (Fig. 6d, h) and left (Fig. 6f, j) synovial membrane presented less hyperplasia, mild inflammatory infiltrate, and consequently a decrease in pannus formation. The alterations in cartilage in the anethole-treated AIA group were also less severe than in the untreated AIA group.

Table 2 shows the mean scores for changes in articular cartilage and inflammatory infiltrate in the synovial membrane 14 and 21 days after the arthritis induction. Treatment with anethole decreased the scores of cartilage damage and inflammatory cells in the left and right joints on both days of evaluation. Figure 7 shows the morphometric analyses—synovial membrane (Fig. 7a, b) and articular cartilage thickness (Fig. 7c, d). The AIA group presented left and right synovial membrane thickness that was two times greater than the normal group on both days of evaluation. No difference in synovial thickness was found between days 14 and 21 in the untreated AIA group. Anethole treatment decreased the thickness of the left (by 40%) and right (by 32%) synovial membrane on day 14 (Fig. 7a) and left (by 47%) and right (by 34%) synovial membrane on day 21 (Fig. 7b) compared with the untreated AIA group.

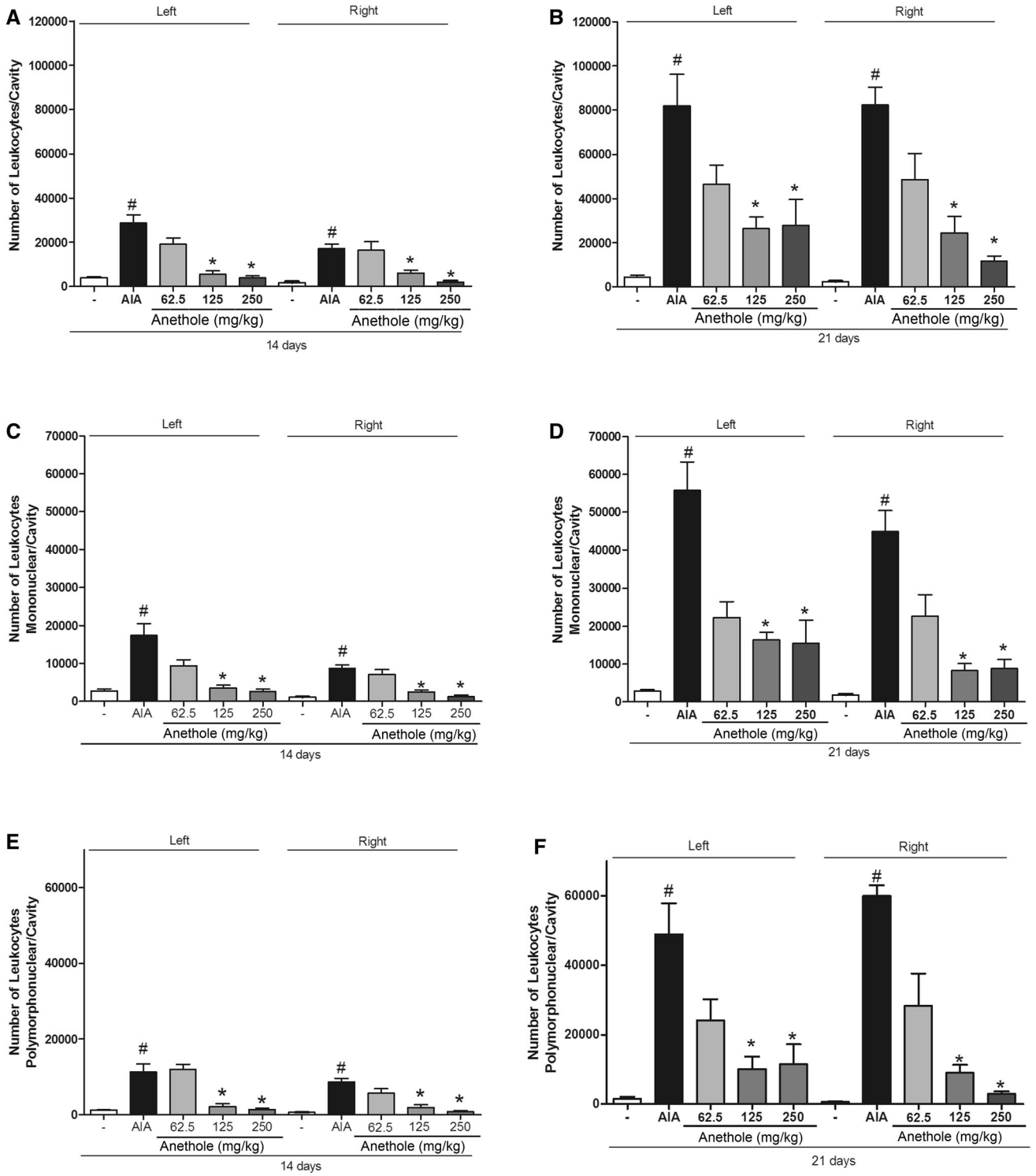

Fig. 2 Effect of anethole (62.5, 125, and 250 mg/kg) on total leukocytes, mononuclear leukocytes, and polymorphonuclear leukocytes 14 days (**a**, **c**, **e**) and 21 days (**b**, **d**, **f**) after the induction of adjuvant-induced arthritis. Anethole was administered daily, orally, beginning on the same day as arthritis induction. The data are expressed as the mean ± SEM of 10 animals for each experimental group. $^{*}p < 0.05$, compared with AIA group; $^{\#}p < 0.05$, compared with normal group (one-way ANOVA followed by Tukey test)

The AIA group exhibited increases in the cartilage joint thickness of the right (20 μm) and left (22 μm) tibia on day 14 and only the right (24 μm) tibia on day 21 after arthritis induction compared with the normal group (16 μm). The thickness of the left joint cartilage of the tibia on day 21 was less (17 μm) than the other days in the anethole-treated

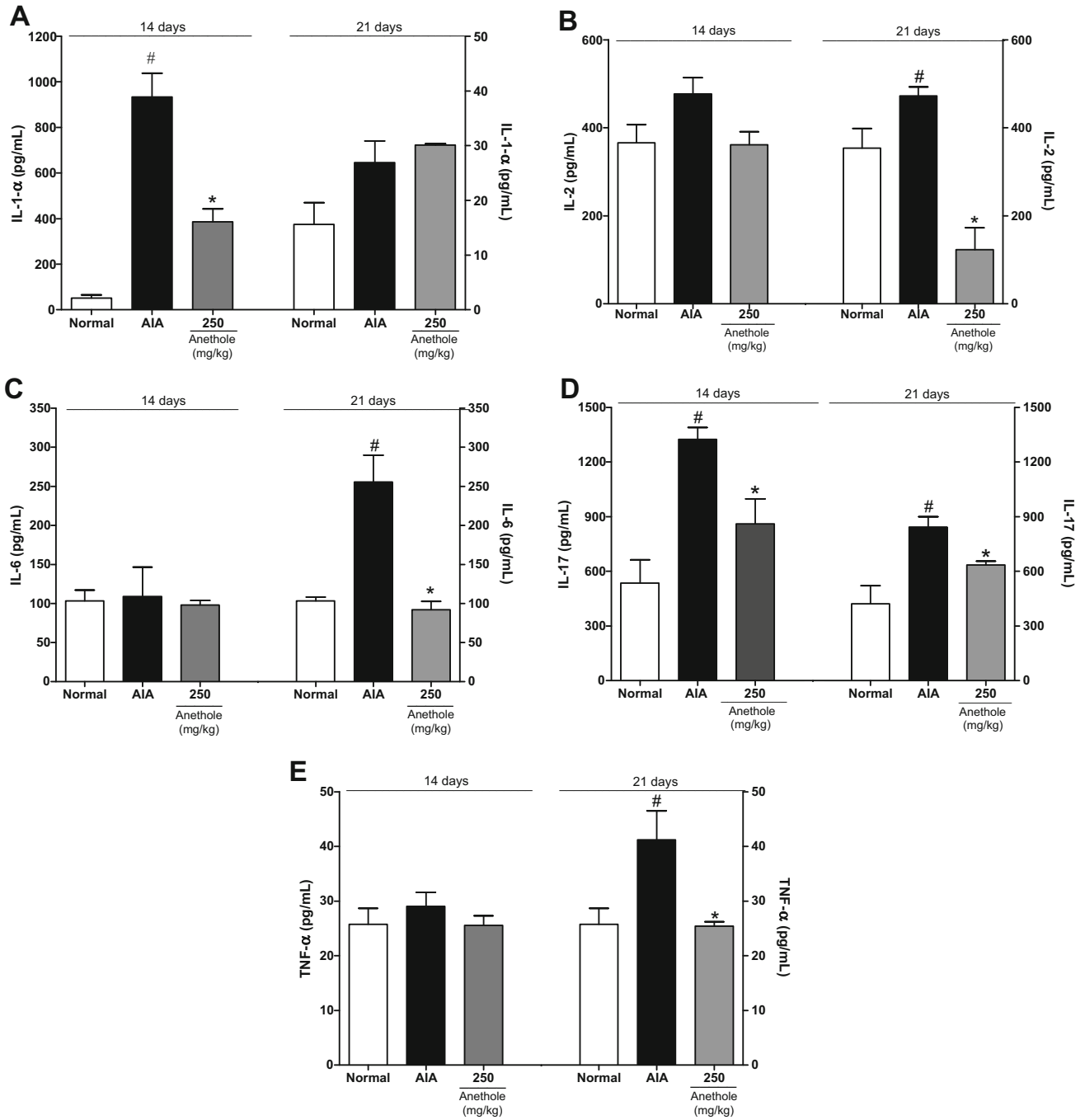

Fig. 3 Effect of anethole (250 mg/kg) on IL-1-α (**a**), IL-2 (**b**), IL-6 (**c**), IL-17 (**d**), and TNF-α (**e**) serum levels 14 and 21 days after the induction of adjuvant-induced arthritis. Anethole was administered daily, orally, beginning on the same day as arthritis induction. The data are expressed as the mean ± SEM of 10 animals. $^{*}p < 0.05$, compared with AIA group; $^{\#}p < 0.05$, compared with normal group (one-way ANOVA followed by Tukey test)

AIA group and decreased to values that were similar to the normal group. The left (21 μm) and right (21 μm) cartilage joint thicknesses on both days of evaluation were similar to the normal group (20 μm; data not shown). Only the cartilage joint of the tibia in the AIA group presented alterations in thickness compared with the normal group in both days. Anethole treatment showed cartilage thickness outcomes similar to AIA group on day 14 (Fig. 6c) and day 21 after arthritis induction, except for the left cartilage thickness that was decreased (24 μm) on day 21 compared to AIA group (Fig. 6d).

Sirius Red-hematoxylin staining showed that the organic matrix area on subcondral bone that underlies the articulation of the tibia and femur was 94.273 μm^2 in the normal

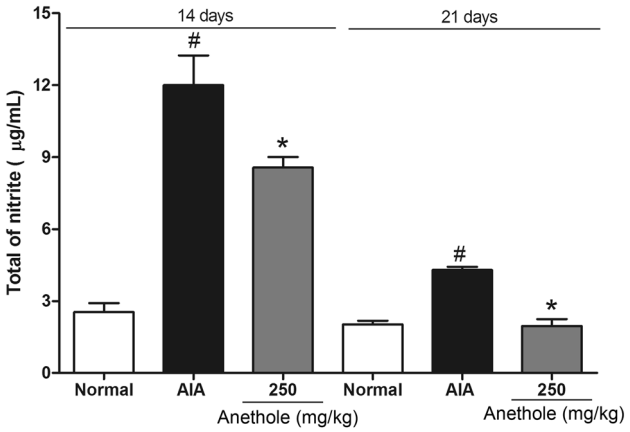

Fig. 4 Effect of anethole (250 mg/kg) on serum nitric oxide levels 14 and 21 days after the induction of adjuvant-induced arthritis. Anethole was administered daily, orally, beginning on the same day as arthritis induction. The data are expressed as the mean ± SEM of 10 animals. $^{*}p < 0.05$, compared with AIA group; $^{\#}p < 0.05$, compared with normal group (one-way ANOVA followed by Tukey test)

group on both the left and right sides on both days 14 and 21. The AIA group exhibited a greater reduction of the organic matrix area (by 48%) on the left and right joints on day 14 (Fig. 8a) and only the left joint on day 21 (Fig. 8b) after arthritis induction. Treatment with anethole contained bone resorption observed in this model showing a high organic matrix area compared with the AIA group. The organic matrix area after anethole treatment decreased bone resorption by 12% (79.660 µm^2) on the left subcondral bone on day 14 and 15% (82.379 µm^2) on day 21 and 10% (84.289 µm^2) on the right subcondral bone on day 21 compared to the AIA group (Fig. 8).

Discussion

The present study evaluated the effects of anethole on AIA in rats. This model is characterized by an intense inflammatory response, with the development of severe local and systemic events, such as hind paw edema (injected with adjuvant or non-injected) secondary lesions, articular leukocyte recruitment, and joint and bone damage. Anethole treatment inhibited the development of the general inflammatory response in arthritic rats. Clinical expression of the disease, such as paw edema and secondary lesions, was reduced after anethole treatment.

The changes that are observed in the AIA model are associated with intense cell migration [21] and pro-inflammatory mediator release [22–24], which induces the expression of adhesion molecules that, together with local cells, exacerbate the inflammatory response [1]. On days 14 and 21 after arthritis induction, although both types of cells markedly increased, there was a prevalence of polymorphonuclear cells. These cells contribute to joint damage through reactive oxygen species, proteolytic enzymes, and cytokine production that, together with macrophages and lymphocytes, amplify the inflammatory response [25].

We found a pronounced decrease in the recruitment of both synovial and systemic cells in anethole treatment group. These outcomes were related to a decrease in the

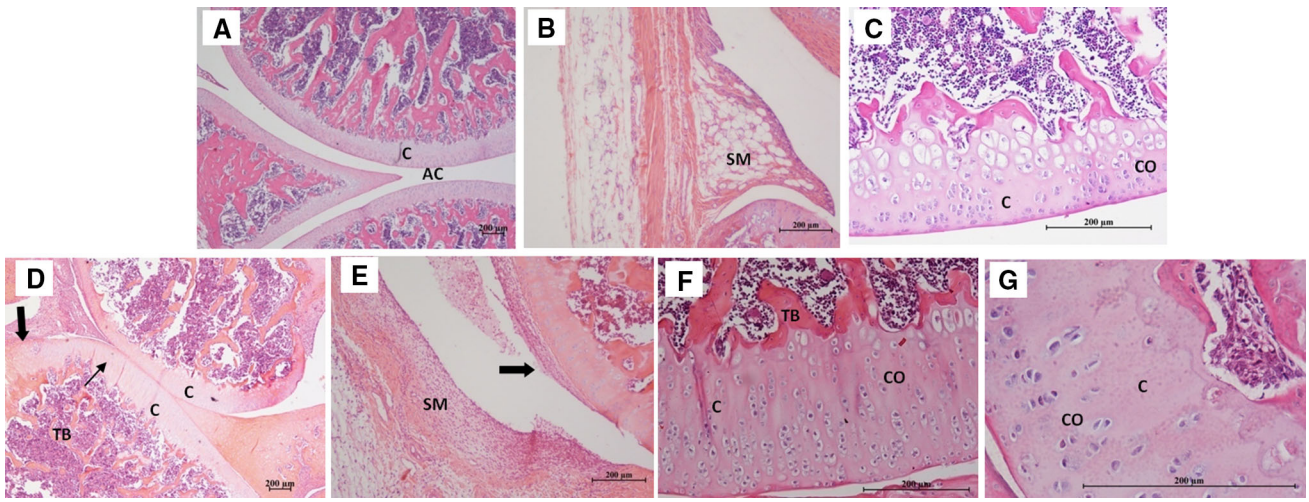

Fig. 5 Photomicrographs of femorotibial articulations in normal rats (**a**–**c**) and rats with adjuvant-induced arthritis (**d**–**g**). (**a**) General aspects of the diarthrose: articular cavity (*AC*) and articular cartilage (*C*) with preserved morphological aspects. **b** Synovial membrane (*SM*) and **c** normal chondrocytes (*CO*) on the articular surface. (**d**–**f**) Arthritic animals on day 14 presented articular cartilage (*C*), thickening of the tibia (*TB*; *thin arrow*), inflammatory infiltrate in the synovial membrane (*SM*; *thick arrow*), and an increase in the number of chondrocytes (*CO*) on the articular surface. **g** Arthritis animals on day 21 presented a decrease in the number of chondrocytes on the articular surface. The images were captured at magnifications of 4× (**a**, **d**), 10× (**b**, **e**), and 20× (**c**, **f**). Hematoxylin/eosin staining

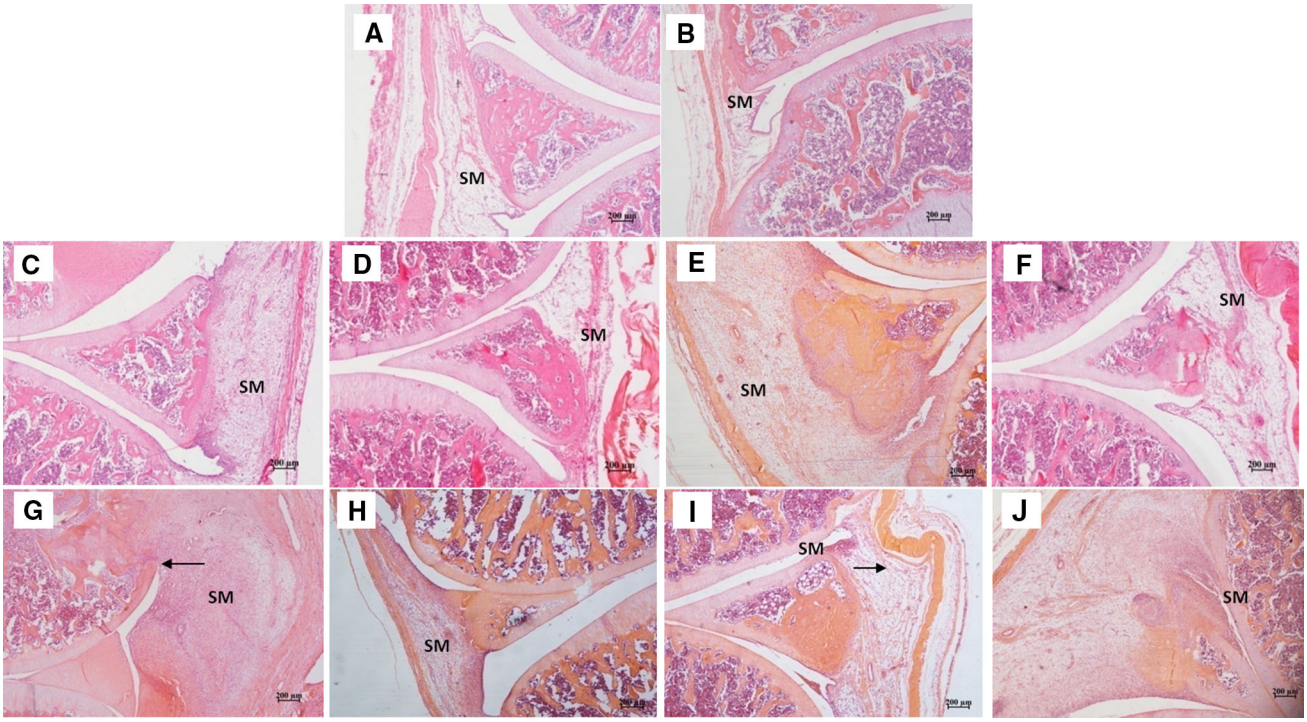

Fig. 6 Photomicrographs of femorotibial articulations in normal rats (**a**, **b**) and rats with adjuvant-induced arthritis on day 14 (**c**–**f**) and day 21 (**g**–**j**) that were treated (**c**, **e**, **g**, **i**) or not treated (**d**, **f**, **h**, **j**) with 250 mg/kg anethole. (**a**, **c**, **d**, **g**, **h**) Left femorotibial articulations. (**b**, **e**, **f**, **i**, **j**) Right femorotibial articulations. Arthritic animals presented marked inflammatory infiltrate, synovial hyperplasia with pannus formation, and invasion of the synovial membrane (*SM*; *arrows*). Anethole decreased inflammatory infiltrate, synovial hyperplasia, and articulations on both days of evaluation. The images were captured at 4× magnification. Hematoxylin/eosin staining

Table 2 Histological scores for alterations in articular cartilage and inflammatory infiltrate in the synovial membrane of the femorotibial articulation 14 and 21 days after the induction of adjuvant-induced arthritis

	Femorotibial articulation							
	Day 14 after AIA				Day 21 after AIA			
	Right		Left		Right		Left	
	Cartilage damage	Inflammatory infiltrate	Cartilage damage	Inflammatory infiltrate	Cartilage damage	Inflammatory infiltrate	Cartilage damage	Inflammatory infiltrate
AIA	4 (3–4)	3 (1–3)	4 (4–5)	3 (1–4)	5 (4–5)	4 (2–4)	5 (4–5)	4 (1–4)
AN 250	2 (0–4)*	1 (0–3)*	1 (0–3)*	1 (0–4)*	3 (4–5)*	2 (0–3)*	1 (0–3)*	1 (0–4)*

Histological scores for the frequency of inflammatory infiltrate in the synovial membrane in femorotibial articulations in rats were graded from 0 to 4 points: (0) absence of inflammatory infiltrate, normal synovial membrane; (1) low inflammatory infiltrate scattered across the tissue; (2) moderate inflammatory infiltrate scattered across the tissue with small groups of cells; (3) high inflammatory cells distributed throughout the tissue; (4) intense inflammatory infiltrate distributed throughout the tissue with evident membrane thickening. Histological scores for cartilage damage in femorotibial articulations in rats was graded from 0 to 5 points: 0 (absence of damage), 1 (increased number of chondrocytes distributed in columns), 2 (increased number of chondrocytes distributed in columns and also disorganized chondrocytes), 3 (decreased number of chondrocytes with disorganized distribution), 4 (change in the number of chondrocytes and disorganized articular membrane superficies), and 5 (change in the number of chondrocytes, disorganized articular membrane superficies, and pannus formation in articular cartilage). The data are expressed as the median (range) for each group

* $p < 0.05$, compared with AIA group (one-way ANOVA followed by Tukey test)

number of joint lymphocytes, attenuation in the inflammation score, and a reduction of pannus formation. The inhibitory effect of anethole on cell migration has been reported previously using different experimental models of acute and persistent inflammation, such as in vitro chemotaxis, in situ microcirculation, and myeloperoxidase determination [11, 12]. However, no studies have investigated the effects of anethole on chronic inflammation, its

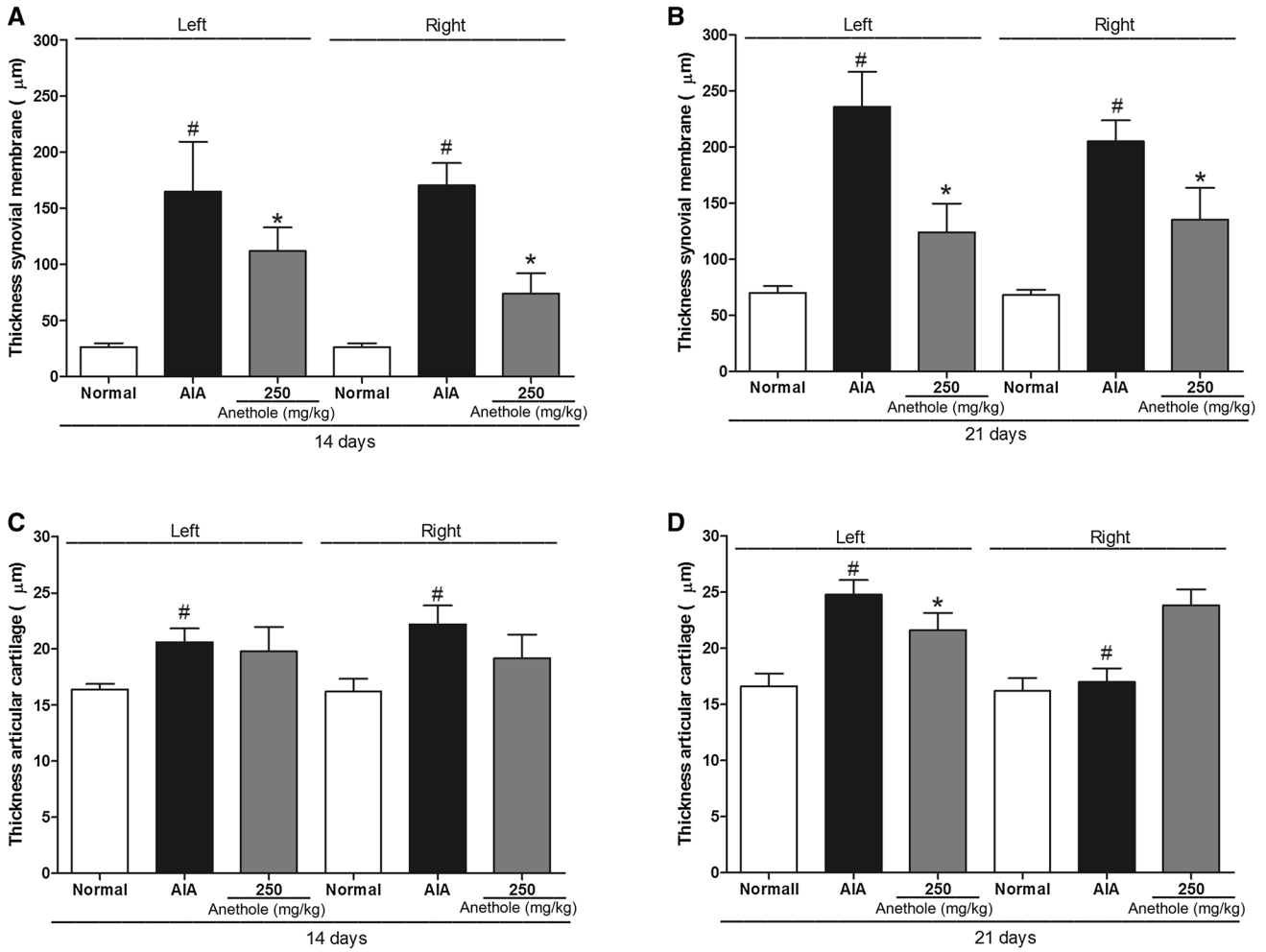

Fig. 7 Thickness of the *left* and *right* synovial membrane 14 days (**a**) and 21 days (**b**) after the induction of adjuvant-induced arthritis and thickness of the *left* and *right* articular cartilage 14 days (**c**) and 21 days (**d**) after the induction of adjuvant-induced arthritis. The data are expressed as the mean ± SEM of 10 animals. $^{*}p < 0.05$, compared with AIA group; $^{\#}p < 0.05$, compared with normal group (one-way ANOVA followed by Tukey test)

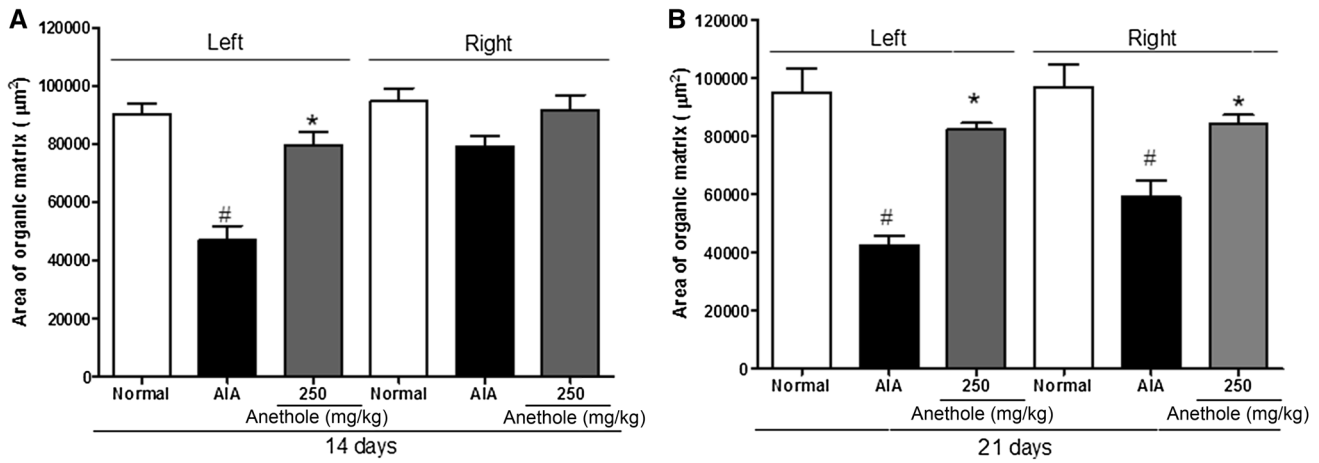

Fig. 8 Organic matrix area of tibial and femoral subcondral bone in normal rats and rats with adjuvant-induced arthritis that were treated or not treated with 250 mg/kg anethole on day 14 (**a**) and day 21 (**b**). Anethole was administered daily, orally, beginning on the same day as arthritis induction. The data are expressed as the mean ± SEM of 10 animals. $^{*}p < 0.05$, compared with AIA group; $^{\#}p < 0.05$, compared with normal group (one-way ANOVA followed by Tukey test)

mechanism of action, and its involvement in bone resorption.

The expression of pro-inflammatory cytokines increases in both serum and tissue in AIA animals. However, the underlying mechanism that is involved in the pathogenesis of the disease remains unknown [2, 26]. The exact roles of specific cytokines are difficult to ascertain in AIA models because of their similar properties and substantial interactions among them [26]. Nonetheless, cytokine levels change according to disease progression, indicating time-dependent cytokine expression in AIA models.

Studies have shown that IL-1, IL-17, and TNF-α levels increase at the beginning of the disease and remain increased on later stages [27–29]. The serum level of IL-6 was increased early [29], although higher during the later phase of the disease [27–29]. We observed high IL-1 and IL-17 levels on day 14 after arthritis induction, with the maintenance of IL-17 levels on day 21. The IL-2, IL-6, and TNF-α levels increased on day 21 in the AIA group. Interestingly, anethole treatment decreased the production/release of IL-1α and IL-17 on day 14 and decreased IL-2, IL-6, IL-17, and TNF-α levels on day 21.

IL-17 is a major cytokine that is involved in stimulating the expression of adhesion molecules, such as intercellular adhesion molecule 1 and vascular cell adhesion molecule 1, which mediate cell recruitment [30, 31]. IL-17 also seems to be involved in both stages of arthritis (acute and chronic) by interfering with synovial cytokine expression, such as IL-6 and TNF-α [21]. TNF-α is produced by monocytes/macrophages and stimulates the expression of other cytokines (IL-1 and IL-6) and adhesion molecules, exacerbating cell migration. IL-6 is the main cytokine that is involved in bone resorption [32]. IL-6, IL-17, and TNF-α together enhance joint and bone damage by increasing receptor activator of NF-κB ligand (RANK) expression in osteoclasts, [23] causing extracellular matrix degradation through metalloproteinase activity [31]. These cytokines are responsible for inflammation and joint damage. In the present study, we found (1) lower levels of TNF- α, IL-6, and IL-17, (2) lower cell migration, (3) and greater changes in joint cartilage/bone tissue. These results suggest that anethole might be a potential modulator of cytokines in the chronic inflammation process.

Reinforcing our dates, we recently found that anethole decreased the synthesis/release of TNF-α and IL-17 in inflammatory acute model [12, 33]. In addition, Sung et al. [34] demonstrated that *Illicium verum* extract, whose main aromatic constituent is anethole (>90%), has important anti-inflammatory effects, reflected by a decrease in TNF-α levels via nuclear factor κB (NF-κB) blockade. NF-κB is the main transcription factor that is responsible for controlling genes that are related to inflammatory diseases [35, 36]. Although we did not assess the NF-κB activity, we may suggest that one possible anti-inflammatory mechanism of anethole is to block the NF-κB, since several cytokines were reduced after its administration.

Nitric oxide also modulates the inflammatory response and joint damage in the AIA model. Nitric oxide is expressed by macrophages, neutrophils, endothelial cells, chondrocytes, and synovial fibroblasts, and it is found in high concentrations in plasma and synovial fluid in RA patients [37, 38]. The experimental model (antigen-induced arthritis) shows that the inhibition of NO synthesis/release in the joint reduces the NO concentration in plasma [39]. Our data showed fewer joint changes and lower nitrite levels in the anethole-treated AIA groups—an undirected marker of NO. Moreover, other studies have reported NO downregulation by anethole treatment [11, 40]. Since, nitric oxide production is controlled by cytokines, such as TNF-α, the reasonable supposition is that the decrease in nitrite levels might be related to the inhibitory effects of anethole on TNF-α [41].

The previous studies have shown that cell migration and pro-inflammatory cytokines in joint tissue are responsible for the activation of local joint cell (chondrocyte) replication at the beginning of arthritis progression [42]. This increase in chondrocytes might be responsible for the joint cartilage thickening that was histological observed on day 14 in the present study (Fig. 6c). However, the increase in cytokine production, mainly IL-6, TNF-α, and NO, coincides with an increase in the catalytic activity of chondrocytes, leading to the degradation of joint cartilage [42], which was observed in the left cartilage in arthritic animals on day 21 (Fig. 6d). Interestingly, anethole was unable to prevent cartilage thickening, but it prevented chondrocyte death, thus decreasing joint degradation. This effect is probably related to the lower inflammatory mediators (NO, IL-17, IL-6, and TNF-α) and cellular infiltrate that were observed on day 21.

Finally, it is important to highlight that anethole has been showing no toxicity effects in the previous studies [12, 43–45] even with high doses or chronic use. In addition, a recent data showed that anethole has a preventive effect against the injury caused by acetaminophen, demonstrating the safety profile of the anethole.

In summary, the present study suggests that anethole has important anti-inflammatory effects and may be considered as a possible option for the treatment of chronic inflammatory diseases, such as RA. Anethole also significantly reduced joint damage and bone resorption. These effects may be related to reductions of the levels of cytokines that are involved in the pathogenesis of arthritis. Although anethole has been shown as a promising arthritis therapy, further studies are necessary to explore the underlying mechanisms of action of this compound.

Acknowledgements The authors are grateful for (a) the technical assistance of Jaílson Araujo Dantas and Célia Regina Miranda, and (b) the financial support of the Conselho Nacional de Desenvolvimento Científico e Tecnológico, Coordenação de Aperfeiçoamento de Pessoal de Nível Superior, and Fundação Araucária-PR.

Compliance with ethical standards

Conflicts of interest The authors declare that there are no conflicts of interest.

References

1. Labranche TP, Jesson MI, Radi ZA, Storer CE, Guzova JA, Bonar SL, et al. JAK inhibition with tofacitinib suppresses arthritic joint structural damage through decreased RANKL production. Arthritis Rheum. 2012;64:3531–42.
2. Feldmann M, Maini SR. Role of cytokines in rheumatoid arthritis: an education in pathophysiology and therapeutics. Immunol Rev. 2008;223:7–19.
3. Roubenoff R, Freeman LM, Smith DE, Abad LW, Dinarello CA, Kehayias JJ. Adjuvant arthritis as a model of inflammatory cachexia. Arthritis Rheum. 1997;40:534–9.
4. Kuncirova V, Ponist S, Mihalova D, Drafi F, Nosal R, Acquaviva A, et al. N-feruloylserotonin in preventive combination therapy with methotrexate reduced inflammation in adjuvant arthritis. Fundam Clin Pharmacol. 2014;28:616–26.
5. Emery P. Treatment of rheumatoid arthritis. BMJ. 2006;332:152–5.
6. Bendele A, Mccomb J, Gould T, Mcabee T, Sennello G, Chlipala E, et al. Animal models of arthritis: relevance to human disease. Toxicol Pathol. 1999;27:134–42.
7. Ramadan G, Al-Kahtani MA, El-Sayed WM. Anti-inflammatory and anti-oxidant properties of Curcuma longa (turmeric) versus Zingiber officinale (ginger) rhizomes in rat adjuvant-induced arthritis. Inflammation. 2011;34:291–301.
8. Chainy GB, Manna SK, Chaturvedi MM, Aggarwal BB. Anethole blocks both early and late cellular responses transduced by tumor necrosis factor: effect on NF-kappaB, AP-1, JNK, MAPKK and apoptosis. Oncogene. 2000;19:2943–50.
9. Chen CH, Degraffenried LA. Anethole suppressed cell survival and induced apoptosis in human breast cancer cells independent of estrogen receptor status. Phytomedicine. 2012;19:763–7.
10. Cho HI, Kim KM, Kwak JH, Lee SK, Lee SM. Protective mechanism of anethole on hepatic ischemia/reperfusion injury in mice. J Nat Prod. 2013;76:1717–23.
11. Domiciano TP, Dalalio MM, Silva EL, Ritter AM, Estevao-Silva CF, Ramos FS, et al. Inhibitory effect of anethole in nonimmune acute inflammation. Naunyn Schmiedebergs Arch Pharmacol. 2013;386:331–8.
12. Ritter AM, Domiciano TP, Verri WA Jr, Zarpelon AC, Da Silva LG, Barbosa CP, et al. Antihypernociceptive activity of anethole in experimental inflammatory pain. Inflammopharmacology. 2013;21:187–97.
13. Caparroz-Assef SM, Bersani-Amado CA, Kelmer-Bracht AM, Bracht A, Ishii-Iwamoto EL. The metabolic changes caused by dexamethasone in the adjuvant-induced arthritic rat. Mol Cell Biochem. 2007;302:87–98.
14. Silva MA, Ishii-Iwamoto EL, Bracht A, Caparroz-Assef SM, Kimura E, Cuman RK, et al. Efficiency of combined methotrexate/chloroquine therapy in adjuvant-induced arthritis. Fundam Clin Pharmacol. 2005;19:479–89.
15. Sukedai M, Ariyoshi W, Okinaga T, Iwanaga K, Habu M, Yoshioka I, et al. Inhibition of adjuvant arthritis in rats by electroporation with interleukin-1 receptor antagonist. J Interferon Cytokine Res. 2011;31:839–46.
16. Naidu VG, Dinesh Babu KR, Thwin MM, Satish RL, Kumar PV, Gopalakrishnakone P. RANKL targeted peptides inhibit osteoclastogenesis and attenuate adjuvant induced arthritis by inhibiting NF-kappaB activation and down regulating inflammatory cytokines. Chem Biol Interact. 2013;203:467–79.
17. Pan R, Dai Y, Gao X, Xia Y. Scopolin isolated from *Erycibe obtusifolia* Benth stems suppresses adjuvant-induced rat arthritis by inhibiting inflammation and angiogenesis. Int Immunopharmacol. 2009;9:859–69.
18. Bersani-Amado CA, Barbuto JAM, Jancar S. Comparative study of adjuvant induced arthritis in susceptible and resistant strains of rats. I. Effect of cyclophosphamide. J Rheumatol. 1990;17:149–52.
19. Cai X, Wong YF, Zhou H, Liu ZQ, Xie Y, Jiang ZH, Bian ZX, Xu HX, Liu L. Manipulation of the induction of adjuvant arthritis in Sprague-Dawley rats. Inflamm Res. 2006;55:368–77.
20. Rosenthale ME. A comparative study of the Lewis and Sprague Dawly rat in adjuvant arthritis. Arch Int Pharmacodyn. 1970;188:14–22.
21. Van Eden W, Waksman BH. Immune regulation in adjuvant-induced arthritis: possible implications for innovative therapeutic strategies in arthritis. Arthritis Rheum. 2003;48:1788–96.
22. Korn T, Bettelli E, Oukka M, Kuchroo VK. IL-17 and Th17 Cells. Annu Rev Immunol. 2009;27:485–517.
23. Pollinger B. IL-17 producing T cells in mouse models of multiple sclerosis and rheumatoid arthritis. J Mol Med (Berl). 2012;90:613–24.
24. Kritas SK, Saggini A, Varvara G, Murmura G, Caraffa A, Antinolfi P, et al. Mast cell involvement in rheumatoid arthritis. J Biol Regul Homeost Agents. 2013;27:655–60.
25. Nurcombe HL, Bucknall RC, Edwards SW. Neutrophils isolated from the synovial fluid of patients with rheumatoid arthritis: priming and activation in vivo. Ann Rheum Dis. 1991;50:147–53.
26. Haddad JJ. Cytokines and related receptor-mediated signaling pathways. Biochem Biophys Res Commun. 2002;297:700–13.
27. Szekanecz Z, Halloran MM, Volin MV, Woods JM, Strieter RM, Kenneth Haines G, et al. Temporal expression of inflammatory cytokines and chemokines in rat adjuvant-induced arthritis. Arthritis Rheum. 2000;43:1266–77.
28. Ferraccioli G, Bracci-Laudiero L, Alivernini S, Gremese E, Tolusso B, De Benedetti F. Interleukin-1beta and interleukin-6 in arthritis animal models: roles in the early phase of transition from acute to chronic inflammation and relevance for human rheumatoid arthritis. Mol Med. 2010;16:552–7.
29. Stolina M, Bolon B, Middleton S, Dwyer D, Brown H, Duryea D, et al. The evolving systemic and local biomarker milieu at different stages of disease progression in rat adjuvant-induced arthritis. J Clin Immunol. 2009;29:158–74.
30. Bessis N, Boissier MC. Novel pro-inflammatory interleukins: potential therapeutic targets in rheumatoid arthritis. Joint Bone Spine. 2001;68:477–81.
31. Ito H, Yamada H, Shibata TN, Mitomi H, Nomoto S, Ozaki S. Dual role of interleukin-17 in pannus growth and osteoclastogenesis in rheumatoid arthritis. Arthritis Res Ther. 2011;13:R14.
32. Pablos Alvarez JL. Interleukin 6 in the physiopathology of rheumatoid arthritis. Reumatol Clin. 2009;5:34–9.
33. Kang P, Kim KY, Lee HS, Min SS, Seol GH. Anti-inflammatory effects of anethole in lipopolysaccharide-induced acute lung injury in mice. Life Sci. 2013;93:955–61.
34. Sung YY, Kim YS, Kim HK. Illicium verum extract inhibits TNF-alpha- and IFN-gamma-induced expression of chemokines and cytokines in human keratinocytes. J Ethnopharmacol. 2012;144:182–9.
35. Barnes PJ, Karin M. Nuclear factor-kappaB: a pivotal transcription factor in chronic inflammatory diseases. N Engl J Med. 1997;336:1066–71.

36. Gilmore TD, Garbati MR. Inhibition of NF-kappaB signaling as a strategy in disease therapy. Curr Top Microbiol Immunol. 2011;349:245–63.
37. Sakaguchi Y, Shirahase H, Ichikawa A, Kanda M, Nozaki Y, Uehara Y. Effects of selective iNOS inhibition on type II collagen-induced arthritis in mice. Life Sci. 2004;75:2257–67.
38. Mcinnes IB, Leung BP, Field M, Wei XQ, Huang FP, Sturrock RD, et al. Production of nitric oxide in the synovial membrane of rheumatoid and osteoarthritis patients. J Exp Med. 1996;184:1519–24.
39. Veihelmann A, Hofbauer A, Krombach F, Dorger M, Maier M, Refior HJ, et al. Differential function of nitric oxide in murine antigen-induced arthritis. Rheumatology (Oxford). 2002;41:509–17.
40. Conforti F, Tundis R, Marrelli M, Menichini F, Statti GA, De Cindio B, et al. Protective effect of Pimpinella anisoides ethanolic extract and its constituents on oxidative damage and its inhibition of nitric oxide in lipopolysaccharide-stimulated RAW 264.7 macrophages. J Med Food. 2010;13:137–41.
41. Amin AR, Attur M, Abramson SB. Nitric oxide synthase and cyclooxygenases: distribution, regulation, and intervention in arthritis. Curr Opin Rheumatol. 1999;11:202–9.
42. Maldonado M, Nam J. The role of changes in extracellular matrix of cartilage in the presence of inflammation on the pathology of osteoarthritis. Biomed Res Int. 2013;2013:284873.
43. Naga Kishore R, Anjaneyulu N, Naga Ganesh M, Sravya N. Evaluation of anxiolytic activity of ethanolic extract of Foeniculum vulgare in mice model. Int J Pharm Pharm Sci. 2012;4:584–6.
44. Badgujar SB, Patel VV, Bandivdekar AH. Foeniculum vulgare Mill: A review of its botany, phytochemistry, pharmacology, contemporary application, and toxicology. Biomed Res Int. 2014;2014:842674-1–842674-32. doi:10.1155/2014/842674.
45. Rocha BA, Ritter AM, Ames FQ, Gonçalves OH, Leimann FV, Bracht L, Natali MR, Cuman RK, Bersani-Amado CA. Acetaminophen-induced hepatotoxicity: preventive effect of trans anethole. Biomed Pharmacother. 2017;86:213–20.